

Chemical pre-processing of cluster galaxies over the past 10 billion years in the IllustrisTNG simulations

Anshu Gupta^{1,2*}, Tiantian Yuan^{2,3†}, Paul Torrey^{4‡}, Mark Vogelsberger^{4§},
 Davide Martizzi⁵, Kim-Vy H. Tran^{2,6,7,8}, Lisa J. Kewley^{1,2}, Federico Marinacci⁴,
 Dylan Nelson⁹, Annalisa Pillepich^{10,11}, Lars Hernquist¹⁰, Shy Genel^{12,13},
 Volker Springel^{14,15,9}

¹Research School of Astronomy and Astrophysics, Australian National University, Canberra, ACT 2611, Australia

²ARC Centre of Excellence for All Sky Astrophysics in 3 Dimensions (ASTRO 3D), Australia

³Centre for Astrophysics and Supercomputing, Swinburne University of Technology, Hawthorn, Victoria 3122, Australia

⁴MIT Kavli Institute for Astrophysics & Space Research, Cambridge, MA, 02139, USA

⁵Department of Astronomy, University of California, Berkeley, CA 94720-3411, USA

⁶School of Physics, University of New South Wales, Kensington, Australia

⁷Australian Astronomical Observatory

⁸George P. and Cynthia W. Mitchell Institute for Fundamental Physics and Astronomy, Department of Physics & Astronomy, Texas A&M University, College Station, TX 77843

⁹Max-Planck-Institut für Astrophysik, Karl-Schwarzschild-Str. 1, 85741 Garching, Germany

¹⁰Harvard-Smithsonian Center for Astrophysics, 60 Garden Street, Cambridge, MA 02138

¹¹Max-Planck-Institut für Astronomie, Königstuhl 17, 69117 Heidelberg, Germany

¹²Center for Computational Astrophysics, Flatiron Institute, 162 Fifth Avenue, New York, NY 10010, USA

¹³Department of Astronomy, Columbia University, 550 West 120th Street, New York, NY 10027, USA

¹⁴Heidelberger Institut für Theoretische Studien, Schloss-Wolfsbrunnengasse 35, 69118 Heidelberg, Germany

¹⁵Zentrum für Astronomie der Universität Heidelberg, Astronomisches Recheninstitut, Mönchhofstr. 12-14, 69120, Heidelberg, Germany

Accepted XXX. Received YYY; in original form ZZZ

ABSTRACT

We use IllustrisTNG simulations to investigate the mass-metallicity relation (MZR) evolution of star-forming cluster galaxies as a function of the formation history of galaxy clusters. The simulations predict enhancement in the gas-phase metallicities of star-forming cluster galaxies ($10^9 < M_* < 10^{10} M_\odot$) at $z \leq 1.0$ compared to field galaxies, consistent with observations. We find that the metallicity enhancement of cluster galaxies appears prior to their infall into the central cluster potential, indicating for the first time a systematic “chemical pre-processing” signature for infalling cluster galaxies. The chemical pre-processing signature is constrained to be ~ 0.05 dex on the MZR and appears below $z \leq 0.5$. Based on the gas inflow rate and the metallicity of the inflowing gas, we identify the pre-enriched gas accretion as a key driver of the chemical evolution in overdense environments, particularly for galaxies in the stellar mass range $10^9 < M_* < 10^{10} M_\odot$. The inflow of pre-enriched gas is effective out to twice the virial radius. Our results motivate future observations looking for pre-enrichment signatures in dense environments.

Key words: galaxies: clusters: general – galaxies: groups: general – galaxies: evolution – galaxies: abundances – method: numerical

1 INTRODUCTION

The chemical abundance of galaxies encodes the cumulative history of baryonic processes such as star formation and gas in-

flow/outflow. Observations clearly show that the cluster environment causes morphological and color transformations of galaxies (e.g., Dressler 1980). However, the impact of cluster-scale overdensities on the chemical evolution of galaxies remains controversial. Observations at $z \sim 0$ find a minimal difference (at most 0.05 dex) in the mass-metallicity relation (MZR) of cluster and field star-forming (SF) galaxies (Ellison et al. 2009; Pasquali et al. 2012; Pilyugin et al. 2017). On the other hand, significant depen-

* E-mail: anshu.gupta@anu.edu.au (AG)

† ASTRO 3D Fellow

‡ Hubble Fellow

§ Alfred P. Sloan Fellow

dencies of the gas-phase metallicity on the cluster-centric distance and the cluster dynamic state are observed (Petropoulou et al. 2012; Gupta et al. 2016). Observations of the MZR at $z > 1.0$ are reported for only a handful of clusters with conflicting results (Tran et al. 2015; Valentino et al. 2015; Kacprzak et al. 2015).

In a hierarchical Λ CDM Universe, massive clusters form through the merger of smaller galaxy groups. Physical properties of group galaxies may be modified prior to accretion onto the main cluster, a process referred to as “pre-processing” (e.g., Zabludoff & Mulchaey 1998; Hou et al. 2014). The most recent observational evidence of pre-processing includes HI-deficiency and quenching of SF in galaxy groups (Brown et al. 2017; Bianconi et al. 2018), though the significance of group pre-processing is debatable (e.g., Berrier et al. 2009). Darvish et al. (2015) find ~ 0.10 dex higher metallicity for galaxies in a filamentary structure at $z \sim 0.5$ than the counterpart field galaxies, suggesting pre-processing role of galaxy filaments on the metallicity. Whether, when and how the chemical abundance of galaxies is altered in the cluster formation history remains an open question.

Current observations are plagued by poorly understood systematic errors such as projection effects, interlopers, selection biases and metallicity diagnostics. These errors can easily overwhelm the chemical enrichment signal as a function of environment, particularly at high redshifts. In addition, the diverse definition of environment makes comparisons across different studies ambiguous (Ellison et al. 2009; Peng & Maiolino 2014). Cosmological simulations with a full 3-dimensional formation history of cluster galaxies are a powerful tool to overcome observational biases and understand the physics of the environmental dependence of the chemical evolution (Davé et al. 2011; Genel 2016; Bahe et al. 2016).

In this Letter, we explore the MZR evolution as a function of the formation history of galaxy groups and clusters in IllustrisTNG, a large-scale cosmological simulation. Using a novel method of separating progenitor cluster galaxies into accreted and infalling categories, we report for the first time a clear systematic signature of “chemical pre-processing” in cluster galaxies over the past 10 Gyrs. We show the effectiveness of pre-enriched gas inflows in driving the chemical evolution of cluster galaxies out to twice the virial radius.

2 METHODS

Our results are based on the IllustrisTNG simulations (Pillepich et al. 2017a; Nelson et al. 2017; Springel et al. 2017; Marinacci et al. 2017; Naiman et al. 2017). The galaxy formation model is an updated and extended version of the Illustris model (Vogelsberger et al. 2013; Torrey et al. 2014). Details of the model modifications are described in Weinberger et al. (2017) and Pillepich et al. (2017b). We use the TNG100 simulation that has a volume of $\sim (100 \text{ Mpc})^3$, $N_{\text{gas}} + N_{\text{DM}} = 2 \times 1820^3$ and $m_b = 1.4 \times 10^6 M_{\odot}$.

From the TNG100 simulation, we select all halos with $M_{200c} \geq 10^{13.0} M_{\odot}$ (total mass enclosed within R_{200c}), leading to a selection of 127 galaxy clusters and groups. The mean cluster halo mass of our sample is $10^{13.4} M_{\odot}$. We define the boundary of a cluster as twice the R_{200c} of the cluster halo, which is similar to the splashback radius (Diemer et al. 2017). Out of all Friends-of-Friends (FOF) subhalos associated with the cluster at $z = 0$, galaxies residing within twice the R_{200c} make up our cluster satellite galaxy sample. Note that we exclude flybys and satellite galaxies in the process of splashing back at $z = 0$ from our analysis.

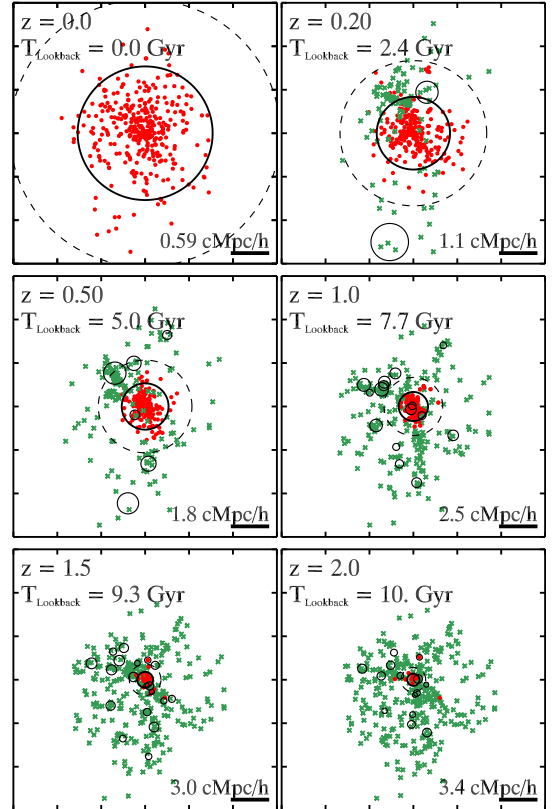


Figure 1. The assembly history of the most massive galaxy cluster ($10^{14.4} M_{\odot}$) in the TNG100 simulation from the projected spatial distribution of cluster members. The red circles and green asterisks represent accreted ($z_{\text{infall}} > z$) and infalling ($z_{\text{infall}} < z$) cluster members respectively. The solid black circles corresponds to the R_{200c} of the dark matter halos associated with the progenitor cluster galaxies. The dashed-black circle represents the cluster boundary ($2 \times R_{200c}$) at each snapshot. All distances are represented in projected comoving scale. Throughout this Letter we present the evolution of physical properties of galaxies in six redshift slices $z = [0.0, 0.2, 0.5, 1.0, 1.5, 2.0]$.

We restrict this analysis to a stellar mass range of $9.0 < \log(M_*/M_{\odot}) < 10.5$ to minimize numerical uncertainties and make predictions that can be clearly observed in the near future. We select 3567 cluster satellite galaxies with stellar mass $9.0 < \log(M_*/M_{\odot}) < 10.5$, without any star formation rates (SFR) cut at $z = 0$. Additional, $\text{SFR} > 0$ cut for cluster satellite galaxies will be enforced during the analysis at any given redshift. Our field galaxy sample consists of 8900 galaxies at $z = 0$ that reside in host halos of mass $M_{200c} < 10^{12.0} M_{\odot}$, have $\text{SFR} > 0$, and $9 < \log(M_*/M_{\odot}) < 10.5$. We focus on the galactic gas-phase metallicity represented in terms of fractional oxygen abundance ($12 + \log(\text{O}/\text{H})$) to facilitate a direct comparison with the nebular metallicity from observations (Torrey et al. 2017). Throughout this Letter the stellar mass and SFR are measured within twice the stellar half mass radius.

We track progenitors of the cluster and field galaxy samples at $z = 0$ using a merger tree catalog based on the technique of Rodriguez-Gomez et al. (2015). At each redshift slice, we use the host halo of the progenitor central cluster galaxy to identify the cluster center and the cluster boundary based on its R_{200c} . We estimate z_{infall} for each progenitor of the present-day cluster satellite galaxy as the earliest time (highest redshift) at which the galaxy

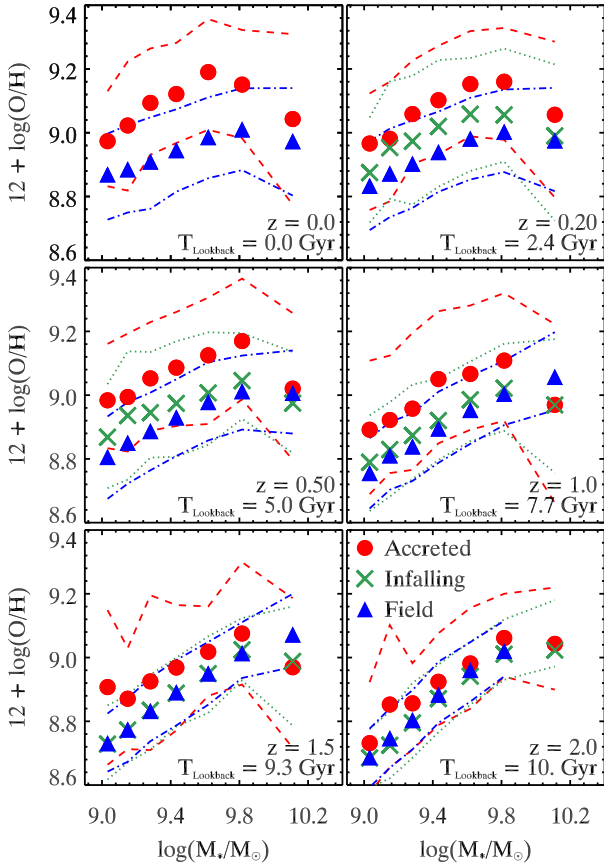


Figure 2. Evolution of the mass-metallicity relation for the accreted cluster (red circles), infalling cluster (green asterisks) and field galaxies (blue triangle). At any given redshift, we are plotting the mean SFR-weighted gas-phase metallicity of galaxies with $\text{SFR} > 0$. The coloured dashed and dotted lines represents the 16th and 84th percentiles. The accreted cluster members show nearly 0.10 – 0.18 dex metal enhancement with respect to field galaxies at each stellar mass bin at $z \leq 1.5$. The infalling cluster members show 0.05 – 0.08 dex metal enhancement with respect to field galaxies at $z \leq 0.5$ suggesting chemical pre-processing of infalling galaxies.

crosses the cluster boundary ($R < 2 \times R_{200c}$ of the central cluster halo) for the first time. Using z_{infall} , we separate progenitor cluster galaxies into two subgroups at each redshift slice: accreted ($z_{\text{infall}} > z$) and infalling ($z_{\text{infall}} < z$) galaxies.

This technique can unambiguously separate the infalling galaxies from the accreted cluster galaxies that are on their second passage into the cluster potential. At each redshift, the progenitors of the field galaxy sample form our comparison sample. Figure 1 shows the assembly history of the most massive cluster in TNG100 ($M_{200c} = 10^{14.4} M_\odot$) through the projected spatial distribution of progenitors at a few redshift snapshots. At high redshift ($z \sim 1.5$), progenitor cluster galaxies have a comoving spatial extent of $\sim 10 - 20 \text{ Mpc}/h$, consistent with the recent work by Chiang et al. (2017).

3 RESULTS

3.1 Cosmic evolution of the mass-metallicity relation with environment

Figure 2 shows the stellar mass versus SFR-weighted gas-phase metallicity for our three galaxy samples (accreted cluster, infalling

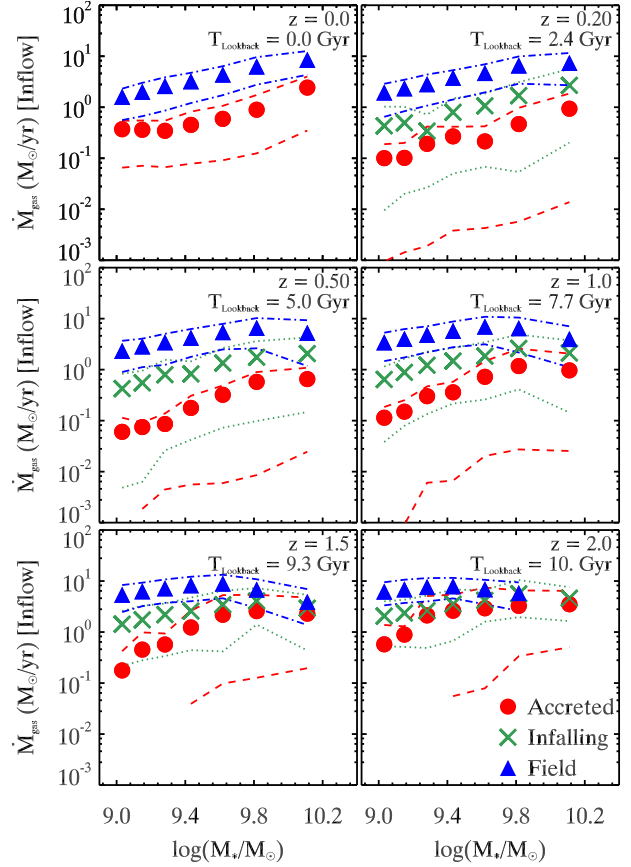


Figure 3. Gas mass inflow rate versus stellar mass for the accreted cluster (red circles), infalling cluster (green asterisks) and field (blue triangles) galaxies. Only star-forming galaxies ($\text{SFR} > 0$) are included in the analysis at any given redshift. The data points represent the mean gas mass inflow rate, and the lines indicate the 16th and 84th percentiles for the respective sample. At each redshift snapshot, cluster satellite galaxies have consistently lower gas inflow rates compared to field galaxies.

cluster, and field) at six different redshifts. From the tracked population of progenitor cluster and field galaxies, we only include galaxies with $\text{SFR} > 0$ at any given redshift. We bin the data by stellar mass such that each stellar mass bin has nearly the same number of galaxies and at least 10 galaxies per bin. The MZR of accreted and infalling galaxies is consistent with the MZR of the field galaxy sample at $z = 2.0$. Signs of the environmental dependence of metallicity emerge around $z = 1.5$, in particular the low mass accreted galaxies ($\log(M_*/M_\odot) < 9.5$) are ~ 0.05 dex more metal-rich compared to counterpart field galaxies. At $z \leq 1.0$, the gas-phase metallicity of accreted cluster galaxies show a consistent metallicity enhancement of 0.15 – 0.20 dex with respect to field galaxies.

The MZR of infalling galaxies lies persistently in between accreted and field galaxies for $z \sim 0-2$, signalling the action of chemical pre-processing in infalling galaxies before they are fully accreted onto their respective clusters. The low mass infalling galaxies ($\log(M_*/M_\odot) < 9.5$) at $z = 0.5$ show an offset of ~ 0.05 dex from the counterpart field galaxies. The metal enhancement permeates to even higher mass infalling galaxies ($\log(M_*/M_\odot) < 10.0$) at $z \sim 0.2$. The infalling galaxies have not crossed the cluster boundary ($2 \times R_{200c}$), hence the metallicity offset between infalling cluster and field galaxies appears prior to infall. Our MZR analysis shows for the first time a systematic signature of chemical pre-

processing in infalling galaxies. In this Letter, we use the term pre-processing more broadly to describe the modification in the properties of galaxies prior to infall onto the main cluster irrespective of their prior group membership.

The MRZ evolution of cluster and field shows a qualitative agreement with observations (Ellison et al. 2009; Pilyugin et al. 2017), though a detailed quantitative comparison with observations is not feasible because of discrepancies in emission line diagnostics (Kewley & Ellison 2008). Most observations find a maximum of 0.05 dex metallicity enhancement for cluster galaxies (Pilyugin et al. 2017), significantly lower than the one predicted by simulations. Contamination by interlopers or infalling galaxies due to projection effects and the lack of dynamic time estimates can easily wash out the metallicity enhancement in observations. Also, a higher SFR cut in observations specifically removes cluster galaxies undergoing change due to the environment. We test different SFR cuts and find a maximum SFR cut of $0.1 M_{\odot}/\text{yr}$ is required to observe the environment driven changes in the metallicity, any higher SFR cut will dilute the observed metallicity enhancement.

The simulation shows a 1-sigma scatter of ~ 0.20 dex in the MZR. The large scatter underlines the cluster-to-cluster variation and shows the challenge of detecting the metallicity enhancement with relatively small cluster samples in observations. Simulations predict no significant evolution in the average metallicity of the highest mass bin ($10.0 < \log(M_*/M_{\odot}) < 10.5$) between $z = 2.0$ to $z = 0.0$ for any galaxy sample. The average metallicity in the highest mass bin is biased towards galaxies with either extremely low SFRs and/or significant AGN contribution, and should be interpreted separately.

3.2 Properties of gas accretion in high-density environment

To understand the origin of the environmental dependence of the MZR and the chemical pre-processing, we investigate the gas accretion history of our three samples using Monte Carlo tracer particles (Genel et al. 2013). At any given redshift, we measure the tracer flux associated with baryons entering the galaxy for the first time over a time interval of 1 Gyr. We then multiply the tracer count with an effective tracer mass to estimate a “raw gas mass inflow rate” (Nelson et al. 2015).

Figure 3 shows the average gas mass inflow rate for the three samples (accreted, infalling and field) in six redshift slices. We find that the gas mass inflow rate is consistently lower by 0.4 – 1.0 dex for accreted and infalling cluster galaxies compared to field galaxies across all redshift slices. The difference in the average gas mass inflow rate between cluster (accreted and infalling) and field galaxies increases slightly with cosmic time, i.e., increases from ~ 0.4 dex at $z = 2.0$ to ~ 1.0 dex at $z < 0.5$. Almost 50% of accreted cluster galaxies with non-zero gas mass inflow rate and SFRs have been accreted onto the main cluster in the past 2 Gyrs. In TNG100, cluster galaxies have on average 0.5 dex lower SFRs than field galaxies at all epochs. Torrey et al. (2017) show that the MZR of field galaxies evolves through either the accretion dominant or enrichment dominant phase.

Figure 4 shows the redshift evolution of the mean metallicity of the inflowing gas. The average metallicity of the baryons associated with the raw gas mass inflow rate is defined as the mean metallicity of inflowing gas. The fractional abundance of all metals used in Figure 4 relates to the fractional oxygen abundance by a simple multiplicative factor. The average metallicity of the inflowing gas increases with cosmic time, irrespective of the galaxy sample or the stellar mass bin. However, galaxies in the cluster environ-

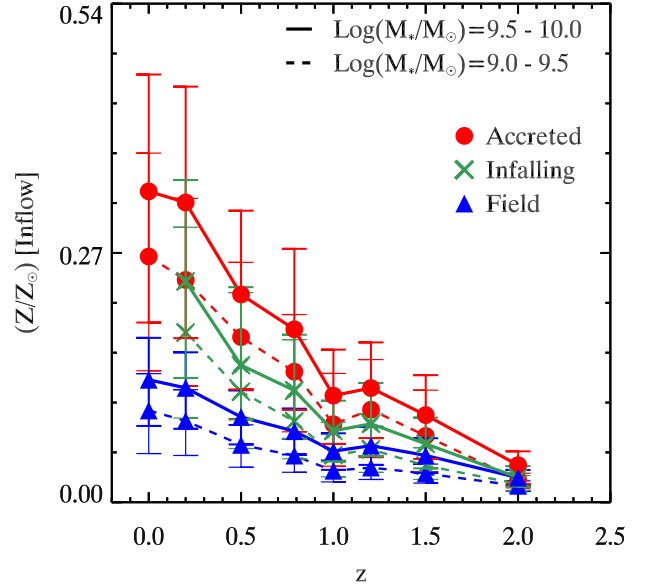


Figure 4. Cosmic evolution of the mean metallicity of the inflowing gas for cluster (red), infalling (green) and field (blue) galaxies. The solid and dashed lines represent galaxies in stellar mass bins labeled in the figure. The inflowing gas for both accreted and infalling cluster galaxies is 2 – 3 times more metal rich at $z = 0$ than field galaxies. Note that we are plotting the total metal content not the fractional oxygen abundance.

ment (accreted or infalling) receive more metal-rich inflowing gas than galaxies in the field, and relatively more so at lower redshifts (Figures 4). Even at $z = 1.5$, accreted cluster galaxies are receiving almost 1.3 times more metal-rich gas than field galaxies; at $z \sim 0$ the difference in metal content can be as large as a factor of 3. Yet, the inflowing gas mass rate is ~ 1.0 dex lower for cluster galaxies than field galaxies. We also find a secondary positive correlation in the metallicity of inflowing gas and the stellar mass, consistent with previous suggestions (Fraternali 2017; Kacprzak et al. 2016).

The average metallicity of the inflowing gas for infalling galaxies continues to lie in-between accreted cluster and field galaxies at all epochs (Figure 4). In fact, at $z < 0.5$, infalling galaxies are accreting 1.5–2 times more metal-rich gas compared to field galaxies. The infalling galaxies have never crossed the boundary of the central cluster potential ($2 \times R_{200c}$) and are receiving metal-rich gas compared to field galaxies, suggesting that enriched gas inflows can be significant at distances larger than $2 \times R_{200c}$. Figure 3 and Figure 4 suggest that the enriched gas inflows contribute significantly to the chemical enrichment of galaxies in overdense environments.

4 DISCUSSION AND CONCLUSION

Using the IllustrisTNG cosmological simulation, we demonstrate the first systematic signature of “chemical pre-processing” of infalling cluster galaxies. We constrain the chemical pre-processing signature to be ~ 0.05 dex in the MZR of infalling galaxies and observable at lower redshifts ($z < 0.5$). The simulation also predicts pre-enrichment of inflowing gas in overdense environments (Figure 4). At $z < 1.0$, inflowing gas for cluster galaxies (infalling or accreted) is 2 – 3 times more metal-rich compared to field galaxies.

Gas removal via gravitational or hydrodynamic interactions in infalling groups has been suspected as the cause of pre-processing

of infalling galaxies. In fact, HI observations of infalling groups reveal Mpc-scale gas trails that are produced by the tidal forces between group members coupled with RPS by the intra-cluster medium (ICM; Cortese et al. 2006; Scott et al. 2015). Our definition of cluster boundary to separate infalling and accreted cluster galaxies is similar to the splashback radius (Diemer et al. 2017). The signature of chemical pre-processing can be used as an observational identification for the splashback radius.

The metallicity enhancement of cluster galaxies on the MZR is qualitatively consistent with observations and recent investigations of cosmological simulations (Davé et al. 2011; Genel 2016; Bahe et al. 2016). Genel (2016) attribute the metallicity enhancement to either the reduced inflow of metal-poor gas or SFR concentration towards the inner, more metal-rich parts for galaxies with stellar mass $\sim 10^{10.3} M_{\odot}$. Observations show that environmental processes are mostly effective for galaxies with $M_{*} < 10^{10} M_{\odot}$ (Peng et al. 2010). Gupta et al. (2017) shows that star formation suppression in the galactic outskirts due to ram pressure stripping (RPS) can not directly produce a significant enhancement in the SFR-weighted metallicity. However, a relative increase in the metallicity of cluster galaxies compared to field galaxies due to suppression of pristine gas inflow by RPS can not be ruled out. We also consistently find lower gas mass inflow rates for both infalling and accreted cluster galaxies compared to field galaxies in the simulation.

The pre-enrichment of the inflowing gas in clusters follows the cosmic evolution of ICM enrichment (Vogelsberger et al. 2017). Peng & Maiolino (2014) also suggested that the mixing of the inflowing gas with the metal-rich ICM can be responsible for the pre-enrichment of inflowing gas in the cluster environment. We speculate that the inflow of pre-enriched gas in combination with the suppression of gas inflows drive the chemical pre-processing of infalling galaxies and the metallicity enhancement of star-forming cluster galaxies. Carefully designed observations are needed to confirm the chemical pre-processing of infalling galaxies and the pre-enrichment signal in overdense environment.

ACKNOWLEDGEMENTS

PT was supported by NASA through Hubble Fellowship grant HST-HF-51384.001-A. MV acknowledges support from a MIT RSC award, the Alfred P. Sloan Foundation, and by NASA ATP grant NNX17AG29G. L.J.K. gratefully acknowledges support from an Australian Research Council (ARC) Laureate Fellowship (FL150100113). T.Y. acknowledges support from an ASTRO 3D fellowship. K. Tran acknowledges support by the National Science Foundation under Grant Number 1410728. Parts of this research were conducted by the Australian Research Council Centre of Excellence for All Sky Astrophysics in 3 Dimensions (ASTRO 3D), through project number CE170100013. The IllustrisTNG simulations and the ancillary runs were run on the HazelHen Cray XC40-system (project GCS-ILLU), Stampede supercomputer at TACC/XSEDE (allocation AST140063), at the Hydra and Draco supercomputers at the Max Planck Computing and Data Facility, and on the MIT/Harvard computing facilities supported by FAS and MIT MKI.

REFERENCES

Bahe Y. M., Schaye J., Crain R. A., McCarthy I. G., Bower R. G., Theuns T., McGee S. L., Trayford J. W., 2016,

- Monthly Notices of the Royal Astronomical Society*, 464, 508
- Berrier J. C., Stewart K. R., Bullock J. S., Purcell C. W., Barton E. J., Wechsler R. H., 2009, *The Astrophysical Journal*, 690, 1292
- Bianconi M., Smith G. P., Haines C. P., McGee S. L., Finoguenov A., Egami E., 2018, *Monthly Notices of the Royal Astronomical Society: Letters*, 473, L79
- Brown T., et al., 2017, *Monthly Notices of the Royal Astronomical Society*, 466, 1275
- Chiang Y.-K., Overzier R. A., Gebhardt K., Henriques B., 2017, *The Astrophysical Journal*, 844, L23
- Cortese L., Gavazzi G., Boselli A., Franzetti P., Kennicutt R. C., O’Neil K., Sakai S., 2006, *Astronomy & Astrophysics*, 453, 847
- Darvish B., Mobasher B., Sobral D., Hemmati S., Nayyeri H., Shivaei I., 2015, *The Astrophysical Journal*, 814, 84
- Davé R., Finlator K., Oppenheimer B. D., 2011, *Monthly Notices of the Royal Astronomical Society*, 416, 1354
- Diemer B., Mansfield P., Kravtsov A. V., More S., 2017, *The Astrophysical Journal*, 843, 140
- Dressler A., 1980, *The Astrophysical Journal*, 236, 351
- Ellison S. L., Simard L., Cowan N. B., Baldry I. K., Patton D. R., McConnachie A. W., 2009, *Monthly Notices of the Royal Astronomical Society*, 396, 1257
- Fraternali F., 2017, *Astrophysics and Space Science Library*, pp 323–353
- Genel S., 2016, *The Astrophysical Journal*, 822, 107
- Genel S., Vogelsberger M., Nelson D., Sijacki D., Springel V., Hernquist L., 2013, *Monthly Notices of the Royal Astronomical Society*, 435, 1426
- Gupta A., Yuan T., Tran K.-V. H., Martizzi D., Taylor P., Kewley L. J., 2016, *The Astrophysical Journal*, 831, 104
- Gupta A., Yuan T., Martizzi D., Tran K.-V. H., Kewley L. J., 2017, *The Astrophysical Journal*, 842, 75
- Hou A., Parker L. C., Harris W. E., 2014, *Monthly Notices of the Royal Astronomical Society*, 442, 406
- Kacprzak G. G., et al., 2015, *The Astrophysical Journal*, 802, L26
- Kacprzak G. G., et al., 2016, *The Astrophysical Journal*, 826, L11
- Kewley L. J., Ellison S. L., 2008, *The Astrophysical Journal*, 681, 1183
- Marinacci F., et al., 2017, preprint (arXiv:1707.03396), 26, 1
- Naiman J. P., et al., 2017, preprint (arXiv:1707.03401), 18, 1
- Nelson D., Genel S., Vogelsberger M., Springel V., Sijacki D., Torrey P., Hernquist L., 2015, *Monthly Notices of the Royal Astronomical Society*, 448, 59
- Nelson D., et al., 2017, preprint (arXiv:1707.03395)
- Pasquali A., Gallazzi A., van den Bosch F. C., 2012, *Monthly Notices of the Royal Astronomical Society*, 425, 273
- Peng Y.-j., Maiolino R., 2014, *Monthly Notices of the Royal Astronomical Society*, 438, 262
- Peng Y.-j., et al., 2010, *The Astrophysical Journal*, 721, 193
- Petropoulou V., Vilchez J., Iglesias-Páramo J., 2012, *The Astrophysical Journal*, 749, 133
- Pillepich A., et al., 2017a, preprint (arXiv:1703.02970), 000
- Pillepich A., et al., 2017b, preprint (arXiv:1707.03406), 000
- Pilyugin L. S., Grebel E. K., Zinchenko I. A., Nefedyev Y. A., Mattsson L., 2017, *Monthly Notices of the Royal Astronomical Society*, 465, 1358
- Rodríguez-Gomez V., et al., 2015, *Monthly Notices of the Royal Astronomical Society*, 449, 49
- Scott T. C., Usero A., Brinks E., Bravo-Alfaro H., Cortese L., Boselli A., Argudo-Fernández M., 2015, *Monthly Notices of the Royal Astronomical Society*, 453, 328
- Springel V., et al., 2017, preprint (arXiv:1707.03397), 23, 1
- Torrey P., Vogelsberger M., Genel S., Sijacki D., Springel V., Hernquist L., 2014, *Monthly Notices of the Royal Astronomical Society*, 438, 1985
- Torrey P., et al., 2017, *MNRAS*, 000, 1
- Tran K.-V. H., et al., 2015, *The Astrophysical Journal*, 811, 28
- Valentino F., et al., 2015, *The Astrophysical Journal*, 801, 132
- Vogelsberger M., Genel S., Sijacki D., Torrey P., Springel V., Hernquist L., 2013, *Monthly Notices of the Royal Astronomical Society*, 436, 3031
- Vogelsberger M., et al., 2017, preprint (arXiv:1707.05318), 21, 1
- Weinberger R., et al., 2017, *Monthly Notices of the Royal Astronomical Society*, 465, 3291

Zabludoff A. I., Mulchaey J. S., 1998, [The Astrophysical Journal](#), 496, 39

This paper has been typeset from a $\text{\TeX}/\text{\LaTeX}$ file prepared by the author.